Journal of Magnetism and Magnetic Materials 427 (2017) 289–295

Contents lists available at ScienceDirect

Journal of Magnetism and Magnetic Materials

journal homepage: www.elsevier.com/locate/jmmm

Effect of immobilized amine density on cadmium(II) adsorption capacities for ethanediamine-modified magnetic poly-(glycidyl methacrylate) microspheres

Tingting Dong[a,b], Liangrong Yang[a,*], Feng Pan[a], Huifang Xing[a], Li Wang[a], Jiemiao Yu[a], Hongnan Qu[a,b,c], Meng Rong[a,b], Huizhou Liu[a,*]

[a] Key Laboratory of Green Process and Engineering, State Key Laboratory of Biochemical Engineering, Institute of Process Engineering, Chinese Academy of Sciences, Beijing 100190, China
[b] University of Chinese Academy of Sciences, Beijing 100049, China
[c] Qingdao Institute of Bioenergy and Bioprocess Technology, Chinese Academy of Sciences, Qingdao 266101, China

ARTICLE INFO

Keywords:
Cadmium
Magnetic
PGMA
EDA
Coordination

ABSTRACT

A series of ethanediamine (EDA) – modified magnetic poly-(glycidyl methacrylate) (m-PGMA-EDA)microspheres with different amine density were synthesized and their cadmium saturation adsorption capacities were examined. The results showed that the cadmium saturation adsorption capacity increased with the immobilized amine density. However, they did not show strong positive linear correlation in the whole range of amine density examined. The molar ratio of amine groups to the adsorbed cadmium decreased with the increase of amine density and eventually reached a minimum value about 4. It suggested that low immobilized amine density led to low coordination efficiency of the amine. It is hypothesized that the immobilized amine groups needed to be physically close enough to form stable amine-metal complex. When the amine density reached to a critical value 1.25 m mol m^{-2}, stable amine-cadmium complex (4:1 N/Cd) was proposed to form. To illustrate the coordination mechanism (structure and number) of amine and Cd, FT-IR spectra of m-PGMA-EDA and m-PGMA-EDA-Cd , and X-ray photoelectron spectroscopy (XPS) of PGMA–EDA and PGMA-EDA-Cd were examined and analyzed.

1. Introduction

Water pollution by heavy metal ions, which are highly carcinogenic and non-biodegradable, may bring long-term threat to the environment and human beings [1–4]. Therefore, it is of great scientific and practical interest to remove heavy metal ions effectively from the wastewaters before they are discharged into the environment. Numerous methods have been used to remove heavy metal ions, including chemical precipitation [5], electrochemical treatment [6], membrane process [7], ion exchange [8], and adsorption [9], etc. Among these methods, adsorption has been proven to be effective and economical, with much less sludge disposal problems [10]. As new promising adsorbent, magnetic polymeric adsorbent with various functional groups has attracted great attention due to the advantages of high separation efficiency and selectivity [11,12]. Magnetic polymeric adsorbent also shows the unique advantage of easy separation under external magnetic field [13].

Amine-functionalized poly-(glycidyl methacrylate)-based polymeric adsorbent, combined PGMA substrate with amine group, has been widely studied for the removal of heavy metal ions [11,14,15]. PGMA has its unique properties like good mechanical strength, sustained acid and base resistance, high reactivity of the epoxy group, and so on. Amine group is considered as one of the most efficient ligands for heavy metal ion complexation. Ethanediamine(EDA), diethylenetriamine(DETA), trithylenetetramine (TETA), and tetraethylenepentamine (TEPA) have been commonly used as the polyamine for PGMA functionalization [16,17]. However, most of the studies focused on the adsorption performance and behavior of amine-functionalized PGMA-based adsorbents in the adsorption of various heavy metal ions. Less attention has been paid to the effect of micro-structure and surface properties of adsorbent on adsorption performance. Once the ligands are immobilized on the solid surface, their distance and space limit will affect their coordination interactions with metal ions.

In a recent study, Liu et al. investigated the removal of copper ions with PGMA beads functionalized with different aliphatic polyamines, including EDA, DETA, TETA, and TEPA [18]. This work is focused on the effect of molecular length and structure of the polyamines on

* Corresponding authors.
E-mail addresses: lryang@ipe.ac.cn (L. Yang), hzliu@ipe.ac.cn (H. Liu).

http://dx.doi.org/10.1016/j.jmmm.2016.10.074
Received 24 June 2016; Received in revised form 12 October 2016; Accepted 16 October 2016
Available online 18 October 2016
0304-8853/

copper ion adsorption performance and their coordination chemistry. Nevertheless, the effect of immobilized amine density on metal ion adsorption capacities has not been considered.

In our work, a series of ethanediamine-modified magnetic poly-(glycidyl methacrylate) microspheres with different amine density was synthesized. And their cadmium saturation adsorption capacities were examined. Our study included (1) effect of the immobilized EDA density on Cd saturation adsorption capacity and (2) the coordination mechanism (structure and number) of amine and Cd on m-PGMA–EDA microspheres surfaces. FT-IR and X-ray photoelectron spectroscopy (XPS) were applied to the further study of Cd ion binding and coordination on m-PGMA–EDA microspheres surfaces.

2. Experimental

2.1. The reagents and materials

Ferrous chloride tetrahydrate ($FeCl_2{\cdot}4H_2O$), ferric chloride hexahydrate ($FeCl_3{\cdot}6H_2O$), ammonium hydroxide ($NH_3{\cdot}H_2O$, 25%, w/w), and ethanediamine (EDA), were of analytical grade and purchased from Xilong Chemical Industry Co. Ltd. (Shantou, China). Glycidyl methacrylate (GMA), polyvinylpyrrolidone (PVP K-30, Mw=40000)were obtained from Sigma–Aldrich Corp. Ltd. (St Louis, MO, USA). Cadmium sulfate octahydrate (≥99.0%) and 2, 2-Azobisisobutyronitrile (AIBN) were purchased from Sinopharm Chemical Reagent Co. Ltd. (Beijing, China). All of the materials were used as received.

2.2. Preparation and characterization of m-PGMA–EDA microspheres

2.2.1. Synthesis of m-PGMA-EDA microspheres

The synthesis route of m-PGMA–EDA microspheres is shown in Scheme 1.

2.2.1.1. Preparation of the PGMA microspheres. PGMA microspheres were prepared by dispersion polymerization according to our previous works [19,20]. First, PVP K-30 (3.1 g, as the stabilizer) was dissolved in a 90% ethanol solution (90 g). Next, GMA (10 g) and AIBN (0.2 g, as the initiator) were dispersed in the solution under a nitrogen atmosphere. The mixture was purged with nitrogen for 30 min and shaft sealed. The polymerization was carried out at 70 °C for 24 h under continuous mechanical stirring (120 rpm). The microspheres were collected by washing several times with distilled water and ethanol and dried in a freezer dryer.

2.2.1.2. In situ coprecipitation of Fe_3O_4 nanoparticles. PGMA microspheres (1 g) were added into 50 mL of a solution containing 1.6 g of $FeCl_3{\cdot}6H_2O$ and 1 g of $FeCl_2{\cdot}4H_2O$ in ice bath. Then the mixture was evacuated under stirring until no further foaming was observed. Next, the microspheres were separated from the mixture by centrifugation and then dispersed in 50 mL of water at 85 °C in a flask equipped with a mechanical stirrer. 10 mL of $NH_3{\cdot}H_2O$ was then added quickly and the mixture was kept stirring under nitrogen for 1 h. The resulting magnetic particles were washed several times with deionized water and ethanol, which were designated as m-PGMA.

2.2.1.3. Reaction with EDA. A series of m-PGMA-EDA microspheres with different amine groups coverage were synthesized by manipulating the concentration of ethylenediamine reacting with m-PGMA microspheres [21,22]. The typical ring-opening reaction of the epoxy groups was carried out as follows: m-PGMA microspheres (2 g) obtained in Section 2.2.1.2 were dispersed into 50 mL of EDA solution, and the mixture was stirred at 80 °C for 12 h. The EDA volume percentage of EDA solution used for preparing m-PGMA-EDA-1, m-PGMA-EDA-2, m-PGMA-EDA-3, m-PGMA-EDA-4, m-PGMA-EDA-5, m-PGMA-EDA-6, m-PGMA-EDA-7 are 1%, 2%, 10%, 20%, 30%, 40%, 55%, respectively. The resulting product was separated with a magnet and washed several times with 0.1 mol L^{-1} HCl solution, ethanol and distilled water and dried in a freezer dryer.

2.2.2. Characterization of m-PGMA-EDA microspheres

The FT-IR spectra were recorded using a Bruker T27 FT-IR spectrophotometer between 4000 and 500 cm^{-1} using the KBr pellet technique, with a resolution of 2 cm^{-1} . The morphology of m-PGMA-EDA microspheres was determined by scanning electron microscopy (SEM, JEOL JSM-6700F, Japan). The particle size distribution, mean diameter and specific surface area of m-PGMA-EDA microspheres were measured by laser diffraction particle size analyzer (Malvern Mastersizer 2000, England). The specific surface area was also measured by BET adsorption method (Quantachrome NOVA3200e, USA). Magnetic properties of m-PGMA and m-PGMA-EDA microspheres were measured by vibrating sample magnetometry (VSM; Model 4 HF VSM, ADE Technologies, USA). X-ray photoelectron spectroscopy (XPS) was performed with a Thermo-Fisher ESCALAB 250Xi imaging X-ray photoelectron spectrometer (Thermo, USA).

Amine capacity was measured by a volumetric method as follows [23]: the microspheres (100 mg) were dispersed in a 0.01 mol L^{-1} HCl solution (100 mL) and incubated at 25 °C for 15 h in a water bath shaker. The residual concentration of HCl was determined by titration against a 0.01 mol L^{-1} NaOH solution and phenolphthalein was chosen as the indicator. Every titration repeated for at least three times and then the data would be averaged. The number of moles of HCl was corresponding to the capacity of the amine groups; therefore, the

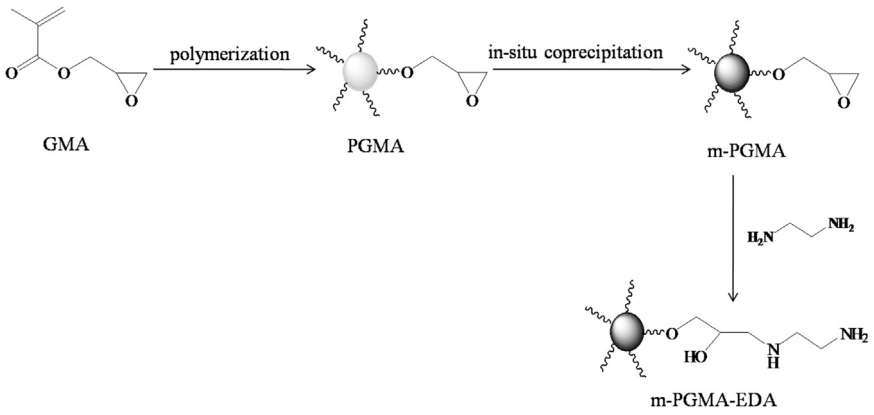

Scheme 1. Preparation of m-PGMA-EDA microspheres.

capacity of the amine groups (mmol g^{-1}) was calculated using the following equation:

$$\text{capacity of the amine groups} = \frac{(c_i - c_e) \times 100}{0.1} \quad (1)$$

Amine density is defined as amine capacity divided by specific surface area of the microspheres.

2.3. Cd adsorption on m-PGMA-EDA microspheres

Cd sorption equilibrium and kinetics were performed on m-PGMA-EDA microspheres in batch experiments. The adsorption experiments were carried out at 25 °C. 10 mg of the adsorbent was added into 20 mL of a solution of known Cd concentration in a 50 mL glass conical flask. Then the flask was placed in a air bath shaker at 200 rpm at 25 °C. The pH value of the system was adjusted by a 0.2 mol L^{-1} NaOH solution and a 0.2 mol L^{-1} HCl solution. Magnetic separation of m-PGMA-EDA microspheres was conducted with a permanent magnet. The concentration of Cd^{2+} ions was analyzed by an inductively coupled plasma optical emission spectrometer (ICP-OES, Perkin Elmer Optima 7000DV, USA). The equilibrium adsorption capacity (q_e, m mol g^{-1}) was calculated using the following equation:

$$q_e = \frac{(C_0 - C_e) \times V}{m} \quad (2)$$

Where C_0 and Ce (m mol L^{-1}) are the initial and equilibrium Cd concentrations in the aqueous solution; V (mL) is the volume of the solution and m (mg) is the adsorbent dose.

Cd saturation adsorption capacities of the prepared m-PGMA-EDA microspheres were achieved by increasing the initial Cd concentrations.

3. Results and discussions

3.1. Characterization of m-PGMA-EDA microspheres

The characterization of m-PGMA-EDA-7 with SEM and laser diffraction particle size analyzer methods was taken as representative of the m-PGMA-EDA series. The SEM photograph of the prepared m-PGMA and m-PGMA-EDA-7 microspheres are shown in Fig. 1(A) and (B), respectively. M-PGMA and m-PGMA-EDA microspheres had a standard spherical form and were monodisperse. The particle size distribution of m-PGMA-EDA microspheres (m-PGMA-EDA-7 as the representative) is shown in Fig. 2. The diameters of m-PGMA and m-PGMA–EDA had a narrow size distribution. The specific surface area(1 is measured by laser diffraction particle size analyzer, 2 is calculated from the BET isotherm of N_2) and mean diameter (1 is obtained from statistics of SEM image, 2 is measured by laser diffraction particle size analyzer) of m-PGMA-EDA microspheres are shown in Table 1.

The magnetic properties of m-PGMA and m-PGMA-EDA were measured by VSM at room temperature. The magnetization curve of m-PGMA and m-PGMA-EDA is shown in Fig. 3. The saturation magnetization of m-PGMA and m-PGMA-EDA was 4.47 emu g^{-1} and 4.34 emu g^{-1}, respectively. No hysteresis, remanence, or coercivity was found, which indicated that m-PGMA and m-PGMA-EDA were superparamagnetic.

The FT-IR spectra of m-PGMA and m-PGMA-EDA microspheres were shown in Fig. 4. In the spectra of m-PGMA and m-PGMA-EDA microspheres, the adsorption bands at 583 cm^{-1} proved the existence of Fe-O [24]. In the spectrum of m-PGMA microspheres, the strong band at 1730 cm^{-1} represented C=O vibrations. And the adsorption bands at 848 and 908 cm^{-1} might be assigned to the epoxy groups on the m-PGMA microspheres [14]. In the spectrum of m-PGMA-EDA microspheres, the adsorption bands at 1604 cm^{-1}, 3310 cm^{-1} and 3360 cm^{-1} corresponding to N-H in the EDA appeared, and the adsorption bands at 848 and 908 cm^{-1} disappeared. The adsorption bands at 1158 cm^{-1} corresponding to CN stretching vibration is also shown in the spectrum of m-PGMA-EDA microspheres [25]. The FT-IR spectra indicated that m-PGMA microspheres had been successfully modified by the EDA.

Amine capacity of m-PGMA-EDA-1 to m-PGMA-EDA-7 measured with the volumetric method are shown in Table 2.

3.2. Adsorption properties of m-PGMA-EDA

The series of m-PGMA-EDA have almost the same chemical properties, therefore, one of them could be chosen as the representative adsorbent to study the effects of pH, contact time, initial ion concentration. Based on our previous work [21], Cd adsorption onto the EDA-modified magnetic PGMA microspheres rose with the increase of pH values, and the maximum adsorption of Cd was observed at pH 6.5. The results were consistent with the metal-amine complexation adsorption mechanism [26,27]. At higher pH, Cd tends to precipitate, which may deteriorate the adsorbent. So the adsorption experiments at higher pH were not conducted. And, the adsorption of Cd onto the EDA-modified magnetic PGMA microspheres reached equilibrium within approximately 1 h. The adsorption data fits the pseudo-second-order model better than the pseudo-first-order model. According to the assumption of the pseudo-second-order model, the adsorption rate of Cd(II) onto the EDA-modified magnetic PGMA microspheres was controlled by chemical processes. Details of the adsorption kinetics are shown in the Supporting information.

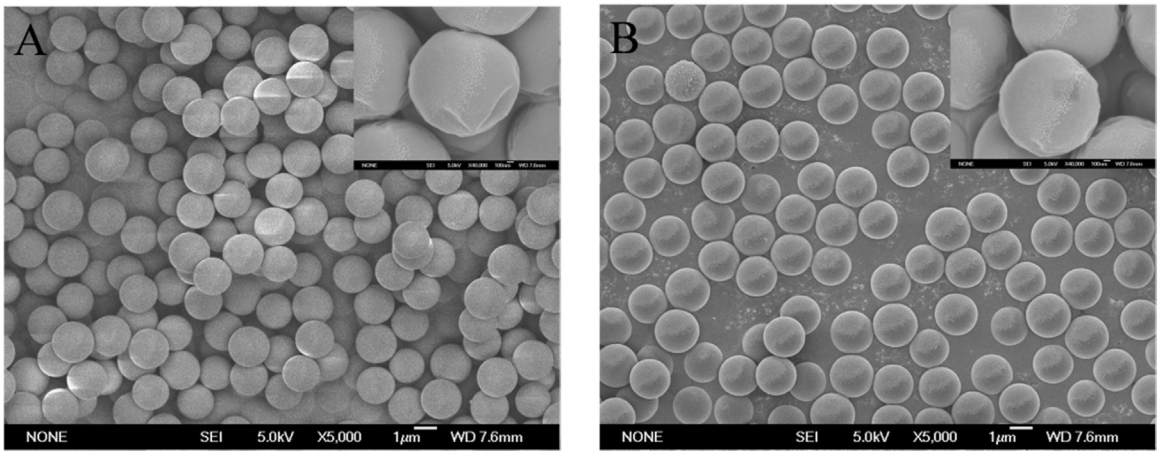

Fig. 1. SEM images of the microspheres: (A) m-PGMA, (B)m- PGMA-EDA-7.

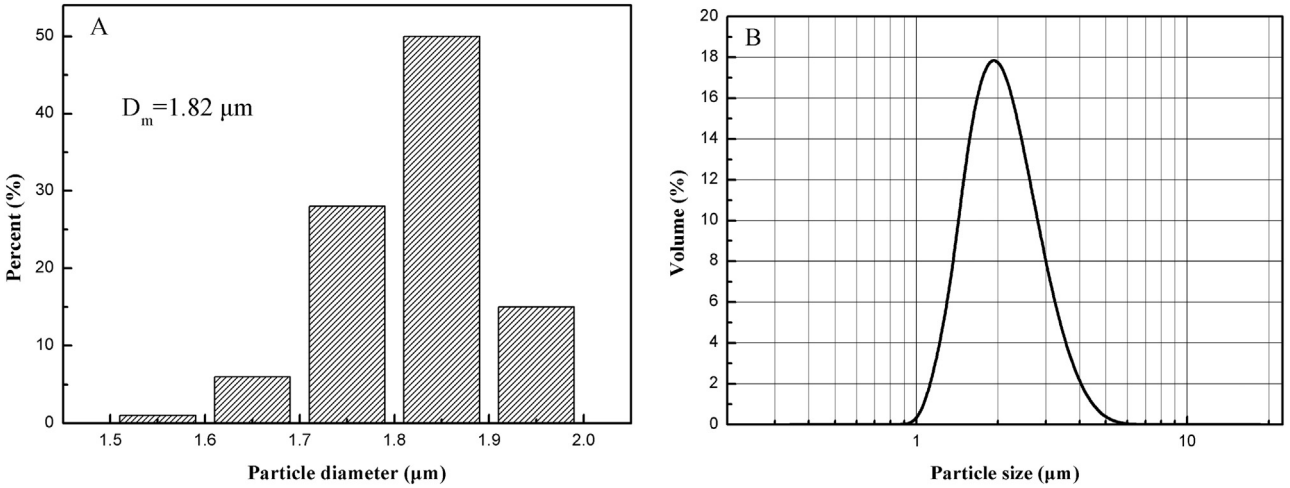

Fig. 2. Size distribution of m-PGMA-EDA-7 obtained from (A) SEM and (B) laser diffraction particle size analyzer.

Table 1
Specific surface area and mean diameter of m-PGMA-EDA-7.

Specific surface area[a] (m^2 g^{-1})	Specific surface area[b] (m^2 g^{-1})	Mean diameter[c] (μm)	Surface weighted mean diameter[d] (μm)	Volume weighted mean diameter[d] (μm)
3.030	3.0	1.82	1.979	2.155

[a] Represent the results measured by laser diffraction particle size analyzer.
[b] Represent the results measured by BET isotherm of N2.
[c] Represent the results obtained from statistics of SEM image.
[d] Represent the results obtained from laser diffraction particle size analyzer.

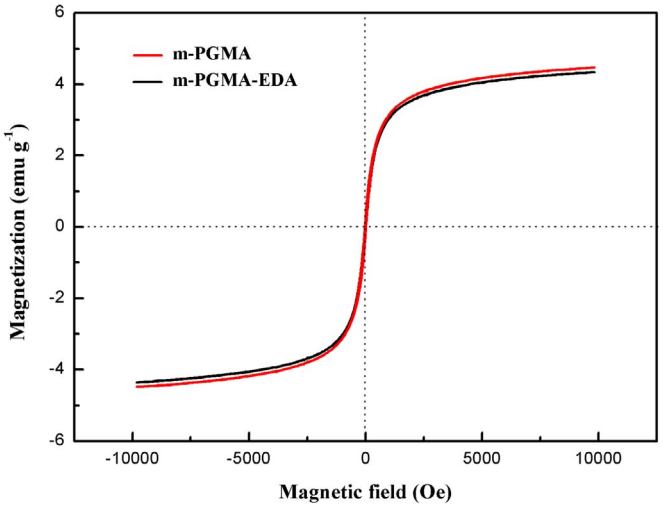

Fig. 3. Magnetization curve of m-PGMA and m-PGMA-EDA-7.

3.3. Effects of the immobilized amine groups capacity on Cd adsorption

The cadmium saturation adsorption capacity of m-PGMA-EDA-1 to m-PGMA-EDA-7 were measured, respectively. The saturation adsorption capacity was attained by increasing the initial Cd concentration. The results were shown in Fig. 5. The cadmium saturation adsorption capacity of m-PGMA-EDA-7 was 1.69 m mol g^{-1} (189.89 mg g^{-1}).

As shown in Fig. 5, the cadmium saturation adsorption capacity increased with the immobilized amine density. However, they did not show strong positive linear correlation in the whole range of amine density examined. The molar ratio of amine groups to adsorbed cadmium decreased with the increase of amine density and reached a minimum value about 4, which meant the formation of 4:1 N/Cd (2:1 EDA/Cd) complex on the solid surface, as presented in Fig. 6. It suggests that low immobilized amine density leads to low effectiveness of the amine. When the amine density reaches a critical value about 1.25 m mol m^{-2} , 4:1 N/Cd complex is proposed to form.

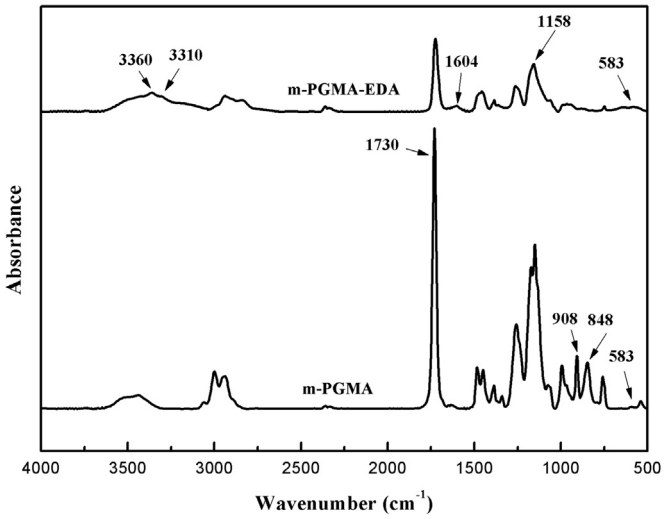

Fig. 4. FT-IR spectra of m-PGMA and m-PGMA-EDA microspheres.

Table 2
Amine capacity and density of m-PGMA-EDA-1 to m-PGMA-EDA-7.

m-PGMA-EDA-n	1	2	3	4	5	6	7
Amine capacity (m mol g^{-1})	1.831	2.442	3.693	4.694	5.087	5.454	7.046
Amine density (m mol m^{-2})	0.604	0.806	1.219	1.549	1.679	1.800	2.325

3.4. The mechanism for the adsorption of Cd on m-PGMA-EDA

To elucidate the mechanism, the FT-IR spectra of m-PGMA-EDA and m-PGMA-EDA-Cd were recorded (Fig. 7), respectively. In the spectrum of m-PGMA-EDA microspheres, the adsorption bands at 1604 cm^{-1}, 3310 cm^{-1} and 3360 cm^{-1} were referred to N-H in the EDA. After loading Cd, these three adsorption bands suffered from changes somehow. The adsorption bands at 3360 cm^{-1} and 3310 cm^{-1} shifted to 3350 cm^{-1} and 3278 cm^{-1}, respectively. And the adsorption band at 1604 cm^{-1} become broader after loading Cd. All these changes

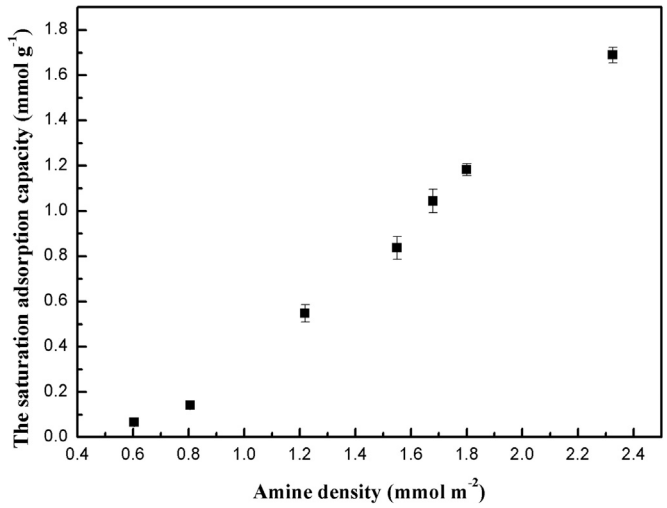

Fig. 5. The cadmium saturation adsorption capacity of m-PGMA-EDA-1 to m-PGMA-EDA-7.

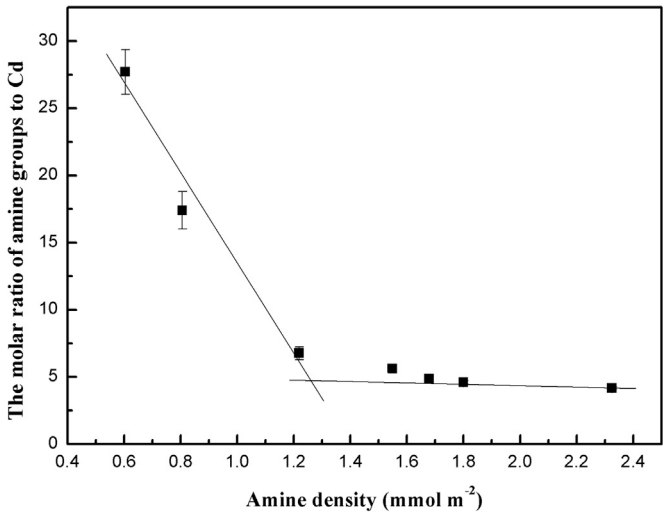

Fig. 6. The molar ratio of amine groups to Cd for m-PGMA-EDA-1 to m-PGMA-EDA-7.

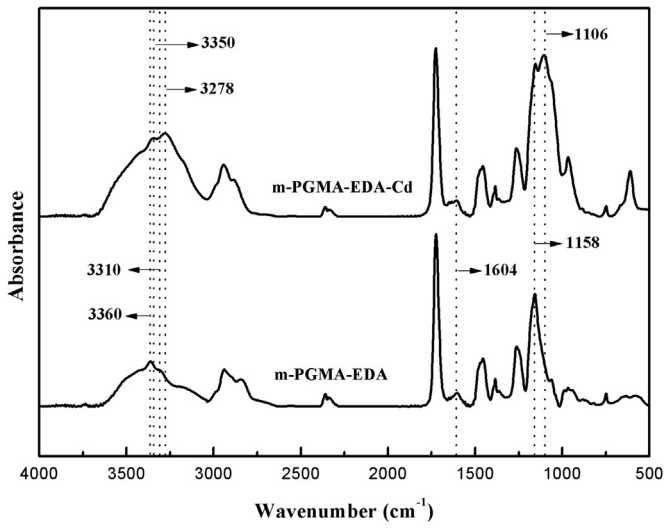

Fig. 7. FT-IR spectra of m-PGMA-EDA and m-PGMA-EDA-Cd.

after cadmium adsorption on m-PGMA-EDA are related to the chemical bonds involving the nitrogen atom. It is also observed that a very strong new band appeared at 1106 cm^{-1} occurred in the FT-IR spectrum of m-PGMA-EDA-Cd in Fig. 7. The peak at 1106 cm^{-1} is highly possible referred to Cd-OH band. As discussed above, we could conclude that cadmium adsorption was mainly through forming the coordination bonds with the amine functional groups and the hydroxyl groups on m-PGMA-EDA microspheres.

To elaborate on the FT-IR results, PGMA-EDA microspheres without magnetism was prepared and the XPS spectra of PGMA-EDA and PGMA-EDA-Cd were examined in Fig. 8. From the wide scans in Fig. 8(A), Cd 3d peaks at 411.5 and 404.7 eV [28] were clearly observed for PGMA-EDA-Cd, in addition to the characteristic peaks of C1s (284.8 eV), N1s (399.0 eV) and O1s (532.0 eV) for the PGMA-EDA [29]. These confirmed the FT-IR results that cadmium were adsorbed onto PGMA-EDA microspheres. To supplement evidence to the FT-IR discovery that the cadmium mainly interacted with the amine functional groups and the hydroxyl groups on PGMA-EDA microspheres during the adsorption process, the XPS C1s, N1s and O1s spectra of PGMA-EDA and PGMA-EDA-Cd are presented in Fig. 8(B–D), respectively. The C1s spectrum of PGMA-EDA shows four peaks at the binding energy of 284.6 eV, 285.4 eV, 286.3 eV and 288.6 eV [Fig. 8(B)] corresponding to carbon in the C-H, C-N, C-O-C and O=C-O, respectively [30,31]. After cadmium adsorption, no obvious changes were found for the C1s spectrum. The N1s spectrum of PGMA-EDA [Fig. 8(C)] showed a peak at 399 eV corresponding to the nitrogen in the neutral amine (-NH_2 or NH) [29,32]. After adsorbing cadmium, the original peak at 399.0 eV shifted to a higher position at 399.1 eV. The shift could be attributable to the nitrogen coordinated with cadmium , thus caused the nitrogen in the amines existing in a more oxidized state.

The O1s spectrum of PGMA-EDA [Fig. 8(D)] showed a peak at 531.9 eV referred to the oxygen in C=O. And a peak at 533.4 eV corresponding to the oxygen in C-OH and C-O-C also existed in the O1s spectrum of PGMA-EDA [31]. After cadmium adsorption, the shoulder in the O1s spectrum of PGMA-EDA disappeared. And the original peaks at 531.9 eV and 533.4 eV shifted to 531.4 eV and 532.8 eV, respectively. These results indicated that the cadmium ion interacted with oxygen in the adsorption process.

The adsorption of cadmium to EDA-modified magnetic PGMA microspheres has been studied at several immobilized amine densities by FT-IR and XPS. The molar ratio of immobilized amine groups to adsorbed cadmium decreased with the increase of amine density and reached a minimum value about 4. It is hypothesized that the immobilized amine groups need to be physically close enough to form stable amine-metal complex. It is possible that the ligands will not be physically close enough to form stable bis (1:2) metal complexes under low immobilized amine groups [33]. When the amine density reaches high enough (a critical amine density: 1.25 m mol m^{-2}), 4:1 N/Cd complex is proposed to form. To sum up all the results, the most possible coordination mechanism of amine and Cd on m-PGMA–EDA microspheres surfaces were illustrated, as shown in Schemes 2 and 3. The chemistry between cadmium ion and immobilized ethanediamine that takes place on the solid surface of PGMA-EDA microspheres is very different from that takes place in solution. When in solution, cadmium ions and ethanediamine is prone to form bis(ethanediamine) cadmium(II) complex at the lower ethanediamine/Cd mole ratio and form tris(ethanediamine)cadmium(II) complex at higher ethanediamine/Cd mole ratio [34–36]. Immobilized ethanediamine is restricted by its limited activity area [33], which is not the same case for free ethanediamine in aqueous solution.

4. Conclusions

In this paper, a series of ethanediamine-modified magnetic poly-(glycidyl methacrylate) microspheres with different amine density were synthesized. And their cadmium saturation adsorption capacities were examined. There were two main findings in this work: (1) The molar ratio of immobilized amine groups to adsorbed cadmium decreased

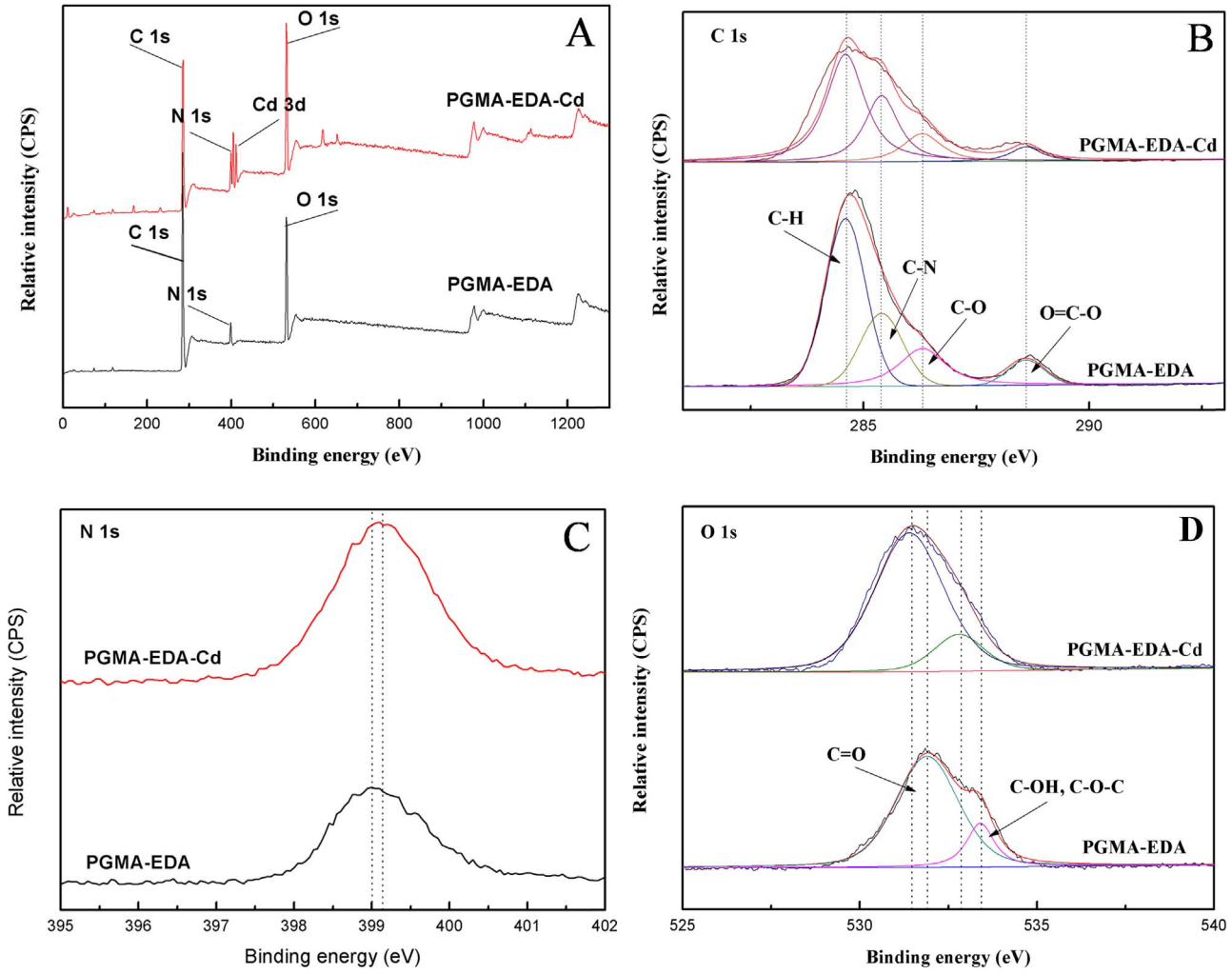

Fig. 8. Wide scans, C1s, N1s and O1s XPS spectra of PGMA-EDA before and after adsorption of Cd(II).

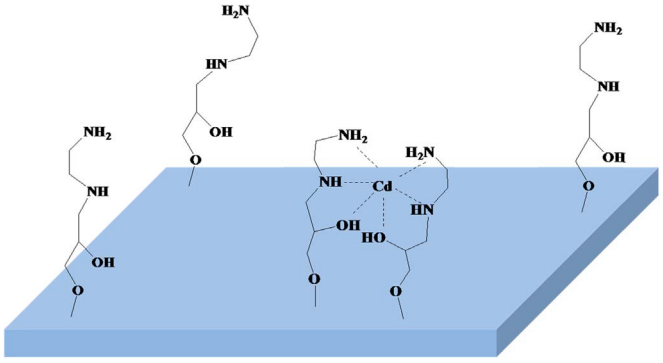

Scheme 2. Diagram depicting idealized complexes structures of Cd and immobilized EDA that would exhibit a N/Cd molar ratio greater than 4.

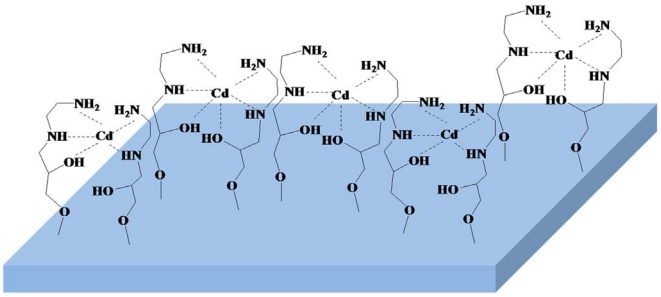

Scheme 3. Diagram depicting idealized complexes structures of Cd and immobilized EDA that would exhibit a N/Cd molar ratio of about 4.

with the increase of amine density and reached a minimum value about 4, illustrating the strong dependence of heavy metal adsorption performance on the immobilized amine density.(2) When the amine density reaches a critical value 1.25 m mol m^{-2} , 4:1 N/Cd (2:1 EDA/Cd) complex is proposed to form, and the hydroxyl also participated in the chelating with Cd. This paper helps to understand the chemistry between metal ion and ligand that takes place on solid surface, which can be very different from that takes place in solution. It is important for the design and preparation of better adsorbents for solid-phase extraction, separation, and preconcentration of metal ions.

Acknowledgements

This work was supported by the National Natural Science Foundation of China (21676273), National Key Natural Science Foundation of China (21136009,U1507203), the National Technology Research and Development Program of China (2015CB251402), the Youth Innovation Promotion Association, CAS (Grant Nos. 2016043), and the Li Foundation USA, Inc.

Appendix A. Supplementary material

Supplementary data associated with this article can be found in the online version at http://dx.doi.org/10.1016/j.jmmm.2016.10.074.

References

[1] B.A. Fowler, Monitoring of human populations for early markers of cadmium toxicity: a review, Toxicol. Appl. Pharmacol. 238 (2009) 294–300.
[2] L. Jarup, Hazards of heavy metal contamination, Br. Med. Bull. 68 (2003) 167–182.
[3] L. Jarup, A. Akesson, Current status of cadmium as an environmental health problem, Toxicol. Appl. Pharmacol. 238 (2009) 201–208.
[4] J. Thompson, J. Bannigan, Cadmium: toxic effects on the reproductive system and the embryo, Reprod. Toxicol. 25 (2008) 304–315.
[5] J. Pavlovic, S. Stopic, B. Friedrich, Z. Kamberovic, Selective removal of heavy metals from metal-bearing wastewater in a cascade line reactor, Environ. Sci. Pollut. Res. 14 (2007) 518–522.
[6] C.L. Yang, Removal of cadmium in leachate from waste alumina beads using electrochemical technology, Chem. Eng. Commun. 189 (2002) 827–848.
[7] O. Genc, L. Soysal, G. Bayramoglu, M.Y. Arica, S. Bektas, Procion green H-4G immobilized poly(hydroxyethylmethacrylate/chitosan) composite membranes for heavy metal removal, J. Hazard. Mater. 97 (2003) 111–125.
[8] S.J. Kim, K.H. Lim, K.H. Joo, M.J. Lee, S.G. Kil, S.Y. Cho, Removal of heavy metal-cyanide complexes by ion exchange, Korean J. Chem. Eng. 19 (2002) 1078–1084.
[9] X.Q. Sun, B. Peng, Y. Ji, J. Chen, D.Q. Li, Chitosan(chitin)/cellulose composite biosorbents prepared using ionic liquid for heavy metal ions adsorption, Aiche J. 55 (2009) 2062–2069.
[10] A. Abbas, A.M. Al-Amer, T. Laoui, M.J. Al-Marri, M.S. Nasser, M. Khraisheh, M.A. Atieh, Heavy metal removal from aqueous solution by advanced carbon nanotubes: critical review of adsorption applications, Sep. Purif. Technol. 157 (2016) 141–161.
[11] D. Duranoglu, I.G.B. Kaya, U. Beker, B.F. Senkal, Synthesis and adsorption properties of polymeric and polymer-based hybrid adsorbent for hexavalent chromium removal, Chem. Eng. J. 181 (2012) 103–112.
[12] Y. Gursel, E. Yavuz, G. Gokay, B.F. Senkal, Preparation of the sulfonamide containing block copolymer as polymeric sorbent for removal of mercury from aqueous solutions, Sep. Sci. Technol. 45 (2010) 2406–2412.
[13] L. Chen, C. Guo, Y. Guan, H. Liu, Isolation of lactoferrin from acid whey by magnetic affinity separation, Sep. Purif. Technol. 56 (2007) 168–174.
[14] L. Niu, S. Deng, G. Yu, J. Huang, Efficient removal of Cu (II), Pb (II), Cr (VI) and As (V) from aqueous solution using an aminated resin prepared by surface-initiated atom transfer radical polymerization, Chem. Eng. J. 165 (2010) 751–757.
[15] A. Gupta, R. Jain, D. Gupta, Studies on uptake behavior of Hg (II) and Pb (II) by amine modified glycidyl methacrylate–styrene–N, N′-methylenebisacrylamide terpolymer, React. Funct. Polym. 93 (2015) 22–29.
[16] H.J. Ma, S.D. Yao, J.Y. Li, C.Q. Cao, M. Wang, A mild method of amine-type adsorbents syntheses with emulsion graft polymerization of glycidyl methacrylate on polyethylene non-woven fabric by pre-irradiation, Radiat. Phys. Chem. 81 (2012) 1393–1397.
[17] Y. Wang, Y. Zhang, C. Hou, X.H. He, M.Z. Liu, Preparation of a novel TETA functionalized magnetic PGMA nano-absorbent by ATRP method and used for highly effective adsorption of Hg(II), J. Taiwan Inst. Chem. Eng. 58 (2016) 283–289.
[18] C. Liu, R. Bai, L. Hong, T. Liu, Functionalization of adsorbent with different aliphatic polyamines for heavy metal ion removal: characteristics and performance, J. Colloid Interface Sci. 345 (2010) 454–460.
[19] W.S. Li, L.R. Yang, H.C. Zhou, X.P. Li, F.C. Wang, X.F. Yang, H.Z. Liu, Gas-assisted superparamagnetic extraction for selective separation of binary mixed proteins, Ind. Eng. Chem. Res. 52 (2013) 16314–16320.
[20] Z.Y. Ma, Preparation and Surface Modification of Magnetic Carriers for Protein Separation and Purification, Institute of Process and Engineering, Beijing, China, 2005 (Ph.D Dissertation).
[21] T. Dong, L. Yang, M. Zhu, Z. Liu, X. Sun, J. Yu, H. Liu, Removal of cadmium (II) from wastewater with gas-assisted magnetic separation, Chem. Eng. J. 280 (2015) 426–432.
[22] Z. Liu, L. Yang, T. Dong, W. Li, X. Sun, M. Zhu, Z. Duan, Q. Liu, H. Liu, Gas-assisted magnetic separation for the purification of proteins in batch systems, Particuology 24 (2016) 170–176.
[23] A. Donia, A. Atia, F. Abouzayed, Preparation and characterization of nano-magnetic cellulose with fast kinetic properties towards the adsorption of some metal ions, Chem. Eng. J. 191 (2012) 22–30.
[24] X.T. Sun, L.R. Yang, Q. Li, Z.N. Liu, T.T. Dong, H.Z. Liu, Polyethylenimine-functionalized poly(vinyl alcohol) magnetic microspheres as a novel adsorbent for rapid removal of Cr(VI) from aqueous solution, Chem. Eng. J. 262 (2015) 101–108.
[25] X. Sun, L. Yang, H. Xing, J. Zhao, X. Li, Y. Huang, H. Liu, High capacity adsorption of Cr (VI) from aqueous solution using polyethylenimine-functionalized poly (glycidyl methacrylate) microspheres, Colloids Surf. A: Physicochem. Eng. Asp. 457 (2014) 160–168.
[26] C.M. Sun, R.J. Qu, C.N. Ji, C.H. Wang, Y.Z. Sun, Z.W. Yue, G.X. Cheng, Preparation and adsorption properties of crosslinked polystyrene-supported low-generation diethanolamine-typed dendrimer for metal ions, Talanta 70 (2006) 14–19.
[27] Q.Y. Liu, Z.X. Ji, Y.L. Bei, Surface-initiated atom transfer radical polymerization of polyamine grafting from magnetic iron oxide submicroparticles for high adsorption capacity of cadmium in aqueous solution, J. Colloid Interface Sci. 394 (2013) 646–651.
[28] G. Hota, S. Idage, K.C. Khilar, Characterization of nano-sized CdS–Ag 2 S core-shell nanoparticles using XPS technique, Colloids Surf. A: Physicochem. Eng. Asp. 293 (2007) 5–12.
[29] C. Liu, R. Bai, Q. San Ly, Selective removal of copper and lead ions by diethylenetriamine-functionalized adsorbent: behaviors and mechanisms, Water Res. 42 (2008) 1511–1522.
[30] C.-C. Teng, C.-C.M. Ma, C.-H. Lu, S.-Y. Yang, S.-H. Lee, M.-C. Hsiao, M.-Y. Yen, K.-C. Chiou, T.-M. Lee, Thermal conductivity and structure of non-covalent functionalized graphene/epoxy composites, Carbon 49 (2011) 5107–5116.
[31] K.K. Lau, K.K. Gleason, Particle Surface Design using an All-Dry Encapsulation Method, Adv. Mater. 18 (2006) 1972–1977.
[32] L. Hernán, J. Morales, J. Santos, J.P. Espinós, A.R. Gonzalez-Elipe, Preparation and characterization of diamine intercalation compounds of misfit layer sulfides, J. Mater. Chem. 8 (1998) 2281–2286.
[33] B. Kannan, D.A. Higgins, M.M. Collinson, Chelation Gradients for Investigation of Metal Ion Binding at Silica Surfaces, Langmuir 30 (2014) 10019–10027.
[34] Z.-X. Deng, C. Wang, X.-M. Sun, Y.-D. Li, Structure-directing coordination template effect of ethylenediamine in formations of ZnS and ZnSe nanocrystallites via solvothermal route, Inorg. Chem. 41 (2002) 869–873.
[35] K. Krishnan, R.A. Plane, Raman and Infrared Spectra of Complexes of Ethylenediamine with Zinc (II), Cadmium (II), and Mercury (II), Inorg. Chem. 5 (1966) 852–857.
[36] T. Fujita, H. Ohtaki, An X-RAY-diffraction study on the structures of Bis(Ethylenediamine)Cadmium(II) and Tris(Ethylenediamine)Cadmium(II) complexes in solution, Bull. Chem. Soc. Jpn. 53 (1980) 930–935.